

**syl- $\alpha$ -D-mannopyranoside (6b) with superoxide** was carried out in the same manner as described above. **6b** (0.13 g, 0.29 mmole) produced a mixture (0.033 g) of four compounds, which are not characterized yet;  $R_f$  0.84 for **6b**, 0.66, 0.41 and 0.34 (toluene : ethyl acetate : ethanol, 5 : 5 : 2);  $^1\text{H-NMR}$  of compounds having  $R_f$  0.41 and 0.34 indicated hydrolysis had occurred.

**5,6-anhydro-3-O-benzyl-1,2-O-isopropylidene- $\beta$ -L-idofuranose (11)** (0.046 g) was obtained from 3-O-benzyl-1,2-O-isopropylidene-5,6-di-O-mesyl- $\alpha$ -D-glucopyranose (**10**) (0.21 g, 0.46 mmole);  $R_f$  0.42 for **10**, 0.59 for **11** (toluene : ethyl acetate, 5 : 3);  $^1\text{H-NMR}$  and  $^{13}\text{C-NMR}$  of **11** were identical to those of the authentic **11** that was synthesized by a known method.<sup>12</sup> (Table 2)

**Acknowledgement.** This work was supported by Research Center for New Bio-Materials in Agriculture, Seoul National University-KOSEF and Academic Foundation of Soong Sil University.

### References

- J. S. Fillipo, Jr., Cheun-Ing Chern, and J. S. Valentine, *J. Org. Chem.*, **40**, 1678 (1975).
- E. J. Corey, K. C. Nicolaou, M. Shibusaki, Y. Machida, and C. S. Shiner, *Tetrahedron Lett.*, **37**, 3183 (1975).
- D. H. Ball and F. W. Parrish, *Advan. Carbohydr. Chem.*, **23**, 233 (1968) and **24**, 139 (1969).
- L. Hough and A. C. Richardson, *Comprehensive Org. Chem.*, (eds. D. H. R. Barton and W. D. Ollis), Vol. **5**, p. 700, Pergamon Press, Oxford (1979).
- K. Bock and C. Pedersen, *Advan. Carbohydr. Chem. and Biochem.*, **41**, 27 (1983).
- N. Baggett, *Carbohydr. Chem.*, (ed. J. F. Kennedy) p. 381, Clarendon Press, Oxford (1988).
- H. H. Baer and D. J. Astles, *Carbohydr. Res.*, **126**, 343 (1984).
- V. S. Rao and A. S. Perlin, *Can J. Chem.*, **59**, 333 (1981).
- N. K. Richtmyer, *Methods in Carbohydr. Chem.*, (eds. R. L. Whistler and M. L. Wolfrom) Vol. **1**, p. 107, Academic Press (1962).
- G. W. J. Fleet, N. M. Carpenter, S. Petursson, and N. G. Ramsden, *Tetrahedron Lett.*, **31**(3), 409 (1990).
- J. E. Nam Shin and A. S. Perlin, *Carbohydr. Res.*, **84**, 315 (1980).
- R. L. Whistler and W. C. Lake, *Methods in Carbohydr. Chem.*, (eds. R. L. Whistler and J. N. BeMiller) Vol. **6**, p. 286, Academic Press (1972).
- J. E. Nam Shin, *Soong Sil Univ., Papers and Essays, Part III. Natural Sciences*, Vol. **13**, 331 (1983).
- Ed. P. M. Collins, *Carbohydrates*, p. 362, Chapman and Hall Chemistry Sourcebooks (1987).
- L. F. Wiggins, *Methods in Carbohydr. Chem.*, (eds. R. L. Whistler and M. L. Wolfrom) Vol. **2**, p. 188, Academic Press (1963).

## Bonding of Electron Deficient Thallium-Metal Cluster Compound

Sungkwon Kang

Department of Chemistry, College of Natural Sciences, Chungnam National University,  
Taejeon 305-764. Received September 8, 1992

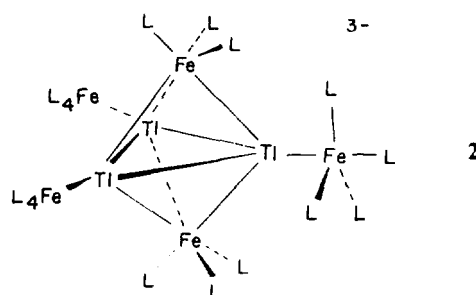
Molecular orbital calculations at the extended Hückel level have been carried out for an electron deficient cluster,  $\text{Ti}_3(\text{FeL}_3)_2(\text{FeL}_4)_3^{-3}$ , where  $\text{L} = \text{CO}$  or  $\text{H}^-$ . The LUMO,  $2a_2''$ , is destabilized by the secondary interaction of the LUMO with  $1a_2''$  on  $(\text{FeL}_3)_2$  fragment. This is one of six skeletal bonding orbitals which are associated with Ti-FeL<sub>3</sub> bonds. Overlap population analysis has been applied to account for two kinds of Ti-Fe bonds. Replacement of the terminal  $\text{C}_3\text{FeL}_4$  by the  $\text{C}_2\text{FeL}_4$  units in cluster results in slight energy stabilization of the cluster.

### Introduction

A large number of clusters with both main group atoms and transition metals have been prepared and structurally determined.<sup>1,2</sup> It is possible to predict the cage geometries of these cluster compounds through a set of electron counting rules.<sup>2,3</sup> The chemical bonding of the cluster compound of  $[\text{Et}_4\text{N}]_6[\text{Ti}_6\text{Fe}_{10}(\text{CO})_{36}]$  (**1**), however, has not been clearly understood yet. From our previous X-ray diffraction study<sup>4</sup>, the inter-Thallium distances were 3.71-3.77 Å, which are in the range of very weak Ti-Ti interactions.<sup>5</sup> In the preliminary calculations the Ti-Ti overlap population was only 0.025.<sup>4</sup> Ti<sup>I</sup>-Ti<sup>I</sup> interaction for the various molecular and solid-state structures was studied by C. Janiak and R. Hoffmann.<sup>6</sup>

In this paper we discuss the analysis of molecular orbital

calculations of compound **1** at the semiempirical extended Hückel level. The simple approach is to consider a dimer of a model system  $\text{Ti}_3(\text{FeL}_3)_2(\text{FeL}_4)_3^{-3}$  (**2**), where  $\text{L} = \text{Two}$  electron donor of CO or  $\text{H}^-$ .



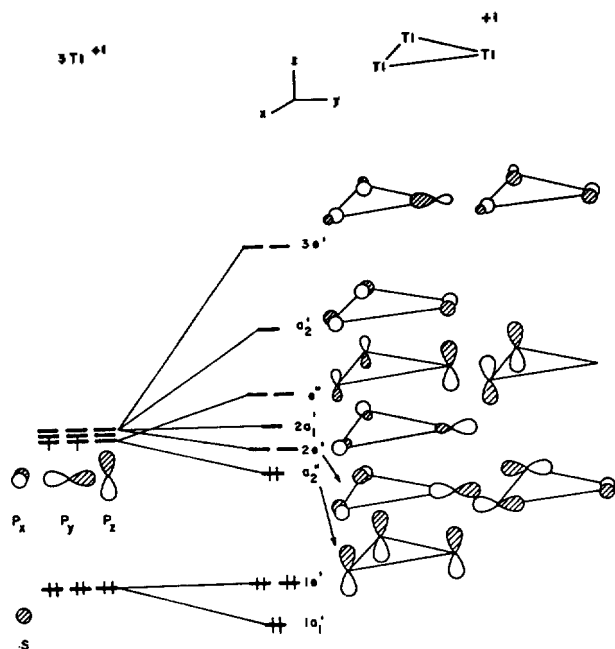


Figure 1. The energy levels of equilateral triangle  $C_{3h}$   $3Tl^{+1}$  fragment.

### The Fragment Orbitals

To investigate the electronic structures of the monomer cluster compound, we divided it into three fragments,  $Tl_3^{+1}$  (3),  $2FeL_3^{-2}$  (4), and  $3FeL_4$  (5). The fragment of  $Tl_3^{+1}$  with symmetry  $D_{3h}$  are shown along with the orbital diagrams in Figure 1.  $Tl_3^{+1}$  is a hypothetical fragment model in the cluster compound.

From the interaction of the three equivalent Tl orbitals in the  $Tl_3^{+1}$  fragments, the energy splitting is not large because of the long inter-Thallium distances (3.71-3.77 Å). Three thallium  $p$  orbitals produce two kinds of fragment orbitals. One is a radial orbital which includes the  $s$  orbitals and the other comprises two tangential orbitals. In Figure 1, the  $a_2''$  orbital is  $\pi$ -type bonding, while the  $e''$  set is  $\pi$ -type orbitals with out-of-phase combination. The  $2e'$  set is the mixtures of tangential and radial  $p$  orbitals. The  $2a_1'$  orbital is made with an in-phase combination of the radial  $p$  orbitals with a small portion of the  $s$  orbitals. At higher energy level is an antibonding  $3e'$  set of  $p$  orbitals mixed with  $s$  orbitals.

As shown in Figure 2, fragment 4 ( $2FeL_3^{-2}$ ) comprises two  $C_{3v}$   $ML_3$  units. The valence MO's for the  $C_{3v}$   $ML_3$  system have already been described in a number of papers.<sup>27</sup> These are shown on the far right and left sides in the figure.

The  $1a_1$  and  $1e$  sets at the low energy levels are pure  $d$  orbitals of Fe atom which correspond to the  $t_{2g}$  set in an octahedral system. In the  $2e$  set the orbitals are primarily metal orbitals of  $d_{yz}$  and  $d_{zx}$  mixed with some  $p$  orbitals which direct toward the missing ligands. The  $2a_1$  is a  $s-p_z$  hybrid orbital of the metal. When two  $C_{3v}$   $FeL_3^{-2}$  fragments are combined together, each fragment orbital interacts in the  $D_{3h}$  symmetry. The low-lying two three-degenerate orbitals ( $1a_1 + 1e$ ), which are shown in the left and right sides of the figure, respectively, form six occupied orbitals of  $1a_1'$ ,

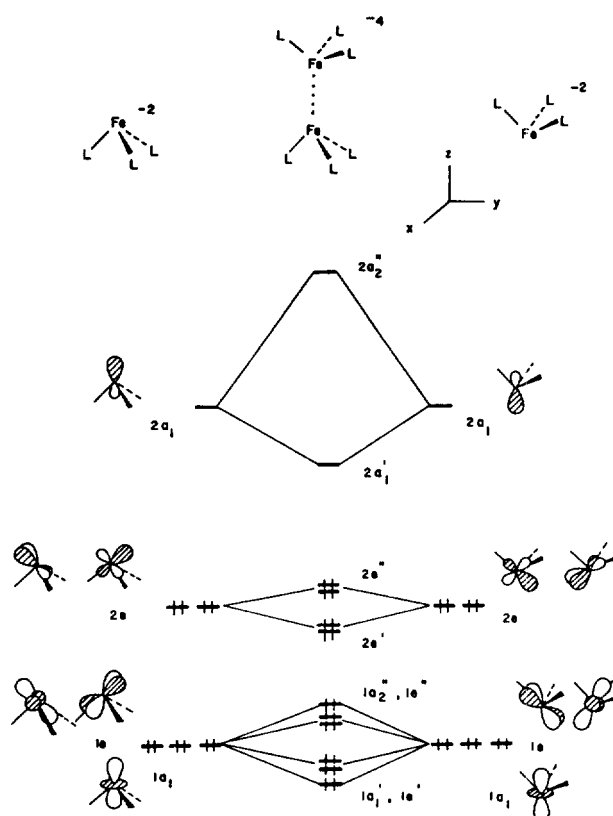


Figure 2. Valence orbitals for an  $2FeL_3^{-2}$  fragment.

$1e'$ ,  $1a_2''$ , and  $1e''$  (shown on the center of the figure). All these orbitals are at the low energy levels with doubly occupied. Therefore, these orbitals cannot interact strongly with the  $Tl_3^{+1}$  fragment orbitals in the cluster compound. The important valence orbitals in the fragment 4 are obtained from the symmetry adapted linear combinations of the three higher orbitals in  $FeL_3^{-2}$ , i.e., the  $2a_1$  and  $2e$  set. In the middle of the figure, the energy levels of the  $2e'$  and  $2e''$  orbitals do not split because of long inter-iron distances (3.13 Å) in the cluster compound. The energy levels of the  $2a_1'$  and  $2a_2''$  orbitals split somewhat because  $4p$  orbitals are more diffusive than  $3d$  orbitals.

Fragment 5,  $3FeL_4$ , is a simple combination of three  $C_{3v}$   $FeL_4$  units in a triangle. The valence orbitals of  $C_{3v}$   $FeL_4$  system can be easily derived from a  $D_{3h}$   $FeL_5$  system. Removing one ligand in axial position,  $a_1'$  orbital is stabilized considerably by forming the  $a_1$  orbital and the hybridization toward the missing ligand (shown in Figure 3).

Two  $e$  sets,  $e'$  and  $e''$ , are not perturbed when one axial ligand is removed. The important valence orbitals in the  $3FeL_4$  fragment are derived from symmetry adapted linear combinations of the two sets of orbitals in  $C_{3v}$   $FeL_4$ , i.e., the  $a_1$  and  $1e$  set. These orbital shapes are shown in top view in 6 and 7.

### The $Tl_3(FeL_3)_2(FeL_4)_3^{-3}$ Cluster Compound

Figure 4 represents the interaction diagram for a  $Tl_3^{+1}$  fragment interacting with two metal fragments.

On the left side of Figure 4 are the orbitals of  $Tl_3^{+1}$ . The

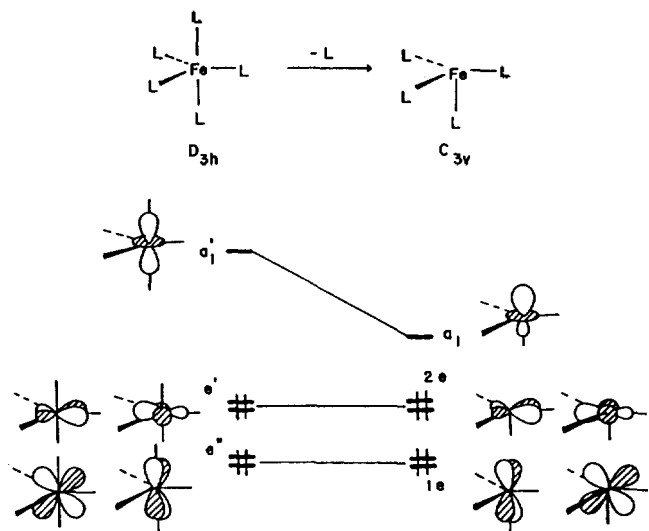
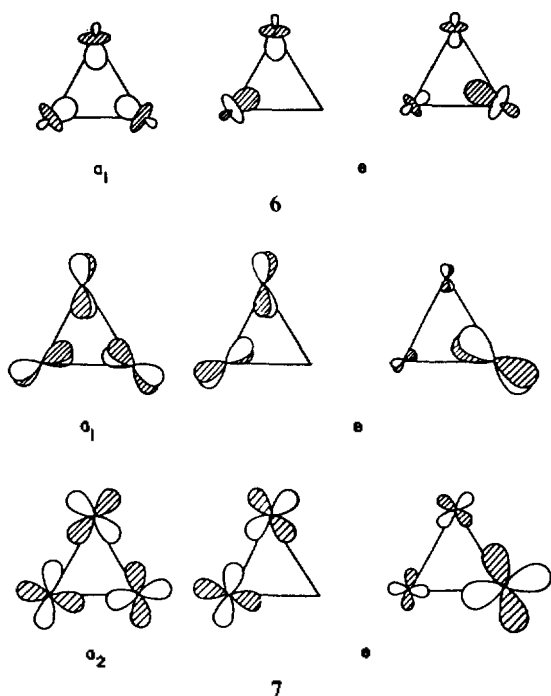


Figure 3. The orbitals of a  $C_{3v}$   $FeL_4$  fragment from a trigonal bipyramidal complex.



$2e'$  on  $Tl_3^{+1}$  strongly interacts with both the  $e'$  on  $2FeL_3^{-2}$  and the  $3e$  set on  $3FeL_4$  to form  $2e'$  molecular orbitals. These molecular orbitals mix with some  $1e'$  orbitals of  $Tl_3^{+1}$  fragment with resulting in an antibonding character. The  $e''$  set on the  $Tl_3^{+1}$  fragment along with the  $e''$  set on  $2FeL_3^{-2}$  unit gives slightly stabilized  $e''$  molecular orbitals in the middle of Figure 4. The  $2a_1'$  orbital of  $Tl_3^{+1}$  interacts primarily with the  $2a_1'$  and  $2a_1$  of the other fragments to produce the highest occupied molecular orbital (HOMO),  $3a_1'$  in cluster compound. According to electron counting rules for cluster compounds,<sup>3</sup> the monomeric molecule 2 with a closo trigonal-bipyramidal geometry should have 12 electrons for skeletal bonding. In the real system, each Tl atom has only one valence electron for skeletal bonding because the other two electrons of Tl atom have been used for the dative bonding

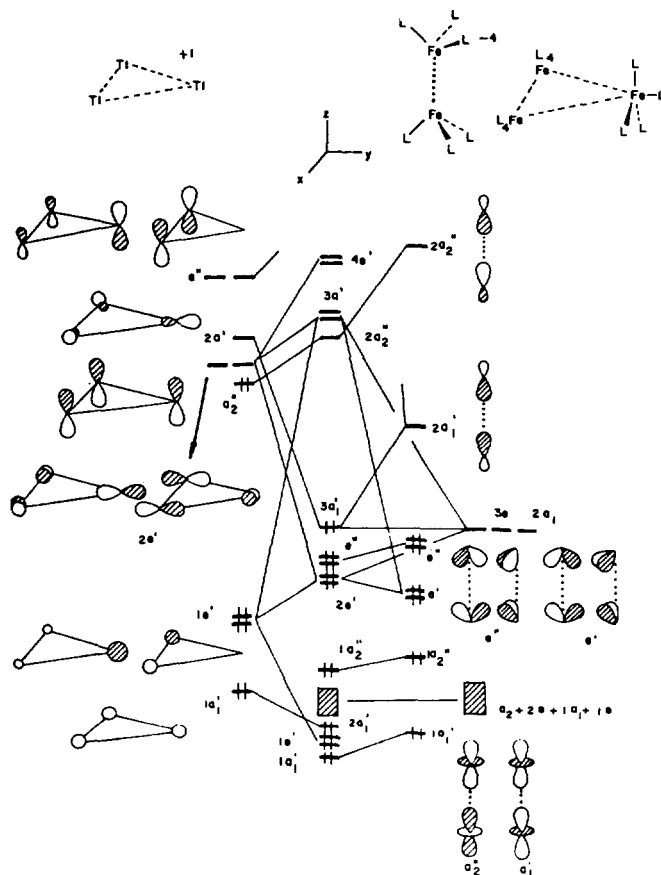
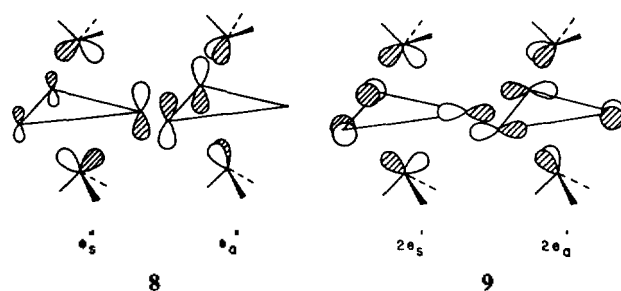
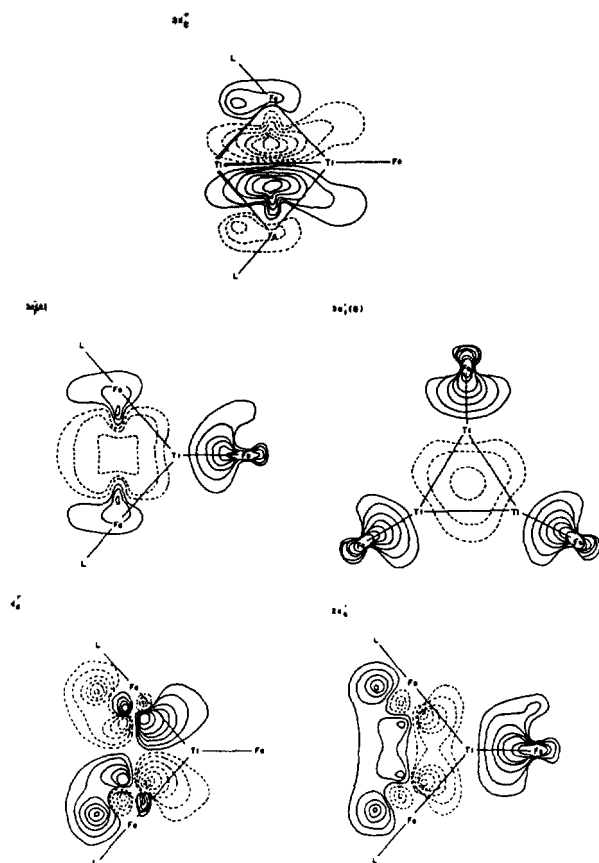


Figure 4. Orbital interaction diagram for the  $Tl_3(FeL_3)_2(FeL_4)_3^{-3}$  cluster compound.

to the  $FeL_4$  fragment. One  $C_{3v}$   $FeL_3$  fragment gives two electrons for skeletal bonding. When the negative charge is considered, these remain 10 electrons for skeletal bonding in cluster. Thus, this cluster is electron deficient. In Figure 4,  $2e'$ ,  $e''$ , and  $3a_1'$  MO's correspond to skeletal bonding with 10 electrons which are associated with Tl- $FeL_3$  bonding. The LUMO,  $2a_2''$  is another skeletal bonding orbital which is destabilized by the secondary interaction of the LUMO with the  $1a_2''$  of  $2FeL_3^{-2}$  unit. The skeletal  $e''$  and  $2e'$  MO's can be represented by 8 and 9, respectively. These are dominant factors to form the bondings between  $2FeL_3^{-4}$  and  $3Tl^{+1}$  units. Contour plots of the selected skeletal MO's are displayed in Figure 5.

The orbitals of the  $e''$  and  $2e'$  sets are plotted on the  $yz$  plane defined in Figure 4. From the contour plots in Figure 5, the orbitals of  $2e_3'$  and  $3a_1'$  have appreciable density on





**Figure 5.** Contour plots of  $2a_2''$ ,  $3a_1'$ ,  $e''$ , and  $2e'$  orbitals in  $Tl_3(FeL_3)_2(FeL_4)_3^{-3}$  cluster. The contours have the values of 0.0125, 0.025, 0.05, 0.075, 0.10, 0.15, and 0.20. The different phases of the wavefunction are represented by full and dashed lines. The orbitals except for  $3a_1'$  (B) have been plotted in the  $yz$  plane which is defined in Figure 4. The  $3a_1'$  (B) orbital has been plotted in  $xy$  plane.

#### FeL<sub>4</sub> fragments.

The computed Tl-Fe (of terminal FeL<sub>4</sub>) overlap populations are 0.120 larger than the others of  $\mu_3$ -FeL<sub>3</sub> units (for which all Tl-Fe distances were fixed to be equal). This difference is consistent with the X-ray observation. Namely, the average distance of the terminal Tl-FeL<sub>4</sub> is 2.54 Å, while that of the bridging Tl-FeL<sub>3</sub> is 2.67 Å. The Tl-Fe overlap population difference can be explained easily. Two interaction types,  $\sigma$ - and  $\pi$ -bonding (10 and 11), are involved in the terminal Tl-FeL<sub>4</sub> bonds.

The filled  $sp$  hybrid orbital of Tl atom strongly interacts with the empty  $s$ ,  $p_y$ , and  $d_{x^2-y^2}$  hybrid orbital of FeL<sub>4</sub> unit in a given coordinate system, shown in 10. And the filled  $d_{xy}$  and  $d_{yz}$  of the terminal FeL<sub>4</sub> unit also interact with empty  $p_x$  and  $p_z$  of Tl atom, 11. These are back-bonding interactions. Total overlap populations from these two interactions are

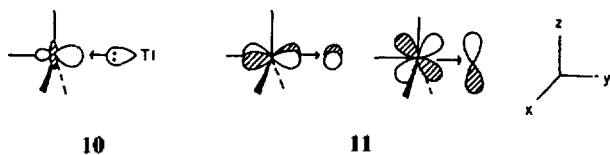


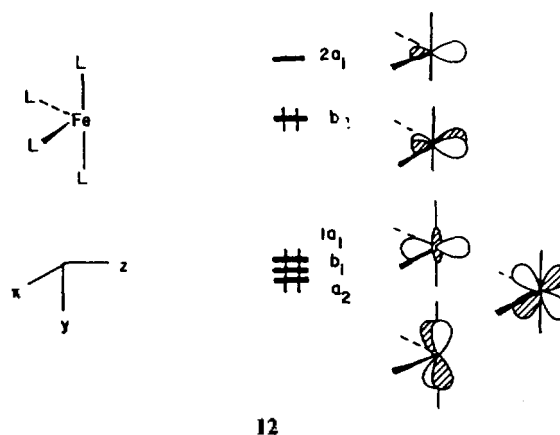
**Table 1.** Parameters Used in the Extended Hückel Calculations

Atom	Orbital	$H_{ii}$ , eV				
		$\zeta_1$	$\zeta_2$	$C_1^a$	$C_2^a$	
Fe	3d	-12.70	5.35	1.80	0.5366	0.6678
	4s	-9.17	1.90			
	4p	-5.37	1.90			
Tl	6s	-11.60	2.30			
	6p	-5.80	1.60			
C	2s	-21.40	1.625			
	2p	-11.40	1.625			
O	2s	-32.30	2.275			
	2p	-14.80	2.275			
H	1s	-13.60	1.30			

<sup>a</sup> Contraction coefficient used in the double- $\zeta$  expansion.

computed to be 0.3453. The main interactions in Tl-FeL<sub>3</sub> are those between the  $s$ ,  $p_z$  orbitals of Tl atoms and the empty  $s$ ,  $p$  orbitals of bridging metal units. The contribution of the metal  $d$  orbital for skeletal bonding is only 16% of total overlap population between the Tl atoms and bridging FeL<sub>3</sub> units.

Many cluster compounds have  $C_{2v}$  ML<sub>4</sub> fragment instead of  $C_{3v}$  ML<sub>4</sub>.<sup>8</sup> This is one of candidates for the replacement of fragment 5, 3FeL<sub>4</sub>. The valence orbitals of  $C_{2v}$  FeL<sub>4</sub> unit are shown in 12.



The overlap populations of 0.3285 between the filled  $sp$  hybrid of Tl atom and LUMO  $2a_1$  in 12 are larger than those of  $C_{3v}$  FeL<sub>4</sub> system, 0.3064. The HOMO  $b_2$  in 12 interacts with empty  $p_x$  of Tl atom. This is back-bonding interaction which is also stronger than  $C_{3v}$  FeL<sub>4</sub> system. Our calculations find that the cluster compound with  $C_{2v}$  FeL<sub>4</sub> unit is slightly more stable than the cluster with  $C_{3v}$ .

**Acknowledgement.** This work was supported by NON DIRECTED RESEARCH FUND, Korea Research Foundation, 1990.

#### Appendix

The calculations have been carried out with the extended Hückel formalism,<sup>9</sup> using the weighted  $H_{ij}$  formalism.<sup>10</sup> The atomic parameters listed in Table 1 were obtained from pre-

vious work.<sup>6,11</sup> In the molecular model, L is a two electron donor, *i.e.*, CO or H<sup>-</sup>. All Ti-Ti, Ti-Fe, Fe-C, Fe-H, and C-O distances were fixed at 3.75, 2.67, 1.78, 1.60, and 1.14 Å, respectively. The L-Fe-L angles were fixed at 90.0°.

### References

- (a) B. F. G. Johnson, "Transition Metal Clusters", Wiley, Chichester, 1980; (b) Ch. Elschenbroich and A. Salzer, "Organometallics", VCH, Weinheim, 1992.
- T. A. Albright, J. K. Burdett, and M.-H. Whangbo, "Orbital Interactions in Chemistry", Wiley, New York, 1985.
- (a) J. K. Burdett, "Molecular shapes", Wiley, New York 1980; (b) K. Wade, *Adv. Inorg. Chem. Radiochem.*, **18**, 1 (1976); (c) D. M. P. Mingos, *Inorg. Chem.*, **24**, 114 (1985); (d) B. K. Teo, *Inorg. Chem.*, **24**, 1627 (1985); (e) W. N. Lipscomb, "In Born Hydride Chemistry", E. L. Muetterties, Ed., Academic Press, New York, pp. 39, 1975.
- K. H. Whitmire, R. R. Ryan, H. J. Wasserman, T. A. Albright, and S. K. Kang, *J. Am. Chem. Soc.*, **108**, 6831 (1986).
- (a) J. Beck and J. Strähle, *Z. Naturforsch.*, **41b**, 1381 (1986); (b) S. Harvey, M. F. Lappert, C. L. Raston, B. W. Skelton, G. Strivastava, and A. H. White, *J. Chem. Soc., Chem. Commun.*, 1216 (1988); (c) K. H. Whitmire, J. M. Cassidy, A. L. Rheingold, and R. R. Ryan, *Inorg. Chem.*, **27**, 1347 (1988); (d) J. M. Cassidy and K. H. Whitmire, *Inorg. Chem.*, **28**, 1432 (1989).
- C. Janiak and R. Hoffmann, *J. Am. Chem. Soc.*, **112**, 5924 (1990).
- (a) T. A. Albright, *Tetrahedron*, **38**, 1339 (1982); (b) K. H. Whitmire, T. A. Albright, S. K. Kang, M. R. Churchill, and J. C. Fettinger, *Inorg. Chem.*, **25**, 2799 (1986); (c) J. A. S. Howell, N. F. Ashford, D. T. Dixon, J. C. Kola, T. A. Albright, and S. K. Kang, *Organometallics*, **10**, 1852 (1991).
- (a) M. R. Churchill, F. J. Hollander, and J. P. Hutchinson, *Inorg. Chem.*, **16**, 2655 (1977); (b) M. R. Churchill and B. G. DeBoer, *Inorg. Chem.*, **16**, 878 (1977); (c) L. F. Dahl and J. F. Blount, *Inorg. Chem.*, **4**, 1965 (1965).
- R. Hoffmann, *J. Chem. Phys.*, **39**, 1397 (1963); R. Hoffmann and W. N. Lipscomb, *J. Chem. Phys.*, **36**, 2179 (1962); **37**, 2872 (1962).
- J. H. Ammeter, H.-B. Bürgi, J. C. Thibeault, and R. Hoffmann, *J. Am. Chem. Soc.*, **100**, 3686 (1978).
- T. A. Albright, P. Hofmann, and R. Hoffmann, *J. Am. Chem. Soc.*, **99**, 7546 (1977).

## Dioxygen Binding to Dirhodium(II, II), (II, III), and (III, III) Complexes. Spectroscopic Characterization of $[\text{Rh}_2(\text{ap})_4(\text{O}_2)]^+$ , $\text{Rh}_2(\text{ap})_4(\text{O}_2)$ , and $[\text{Rh}_2(\text{ap})_4(\text{O}_2)]^-$ , where ap=2-anilinopyridinate Ion

Jae-Duck Lee\*, Chao-Liang Yao, Françoise J. Capdevielle, Baocheng Han, John L. Bear<sup>†</sup>, and Karl M. Kadish<sup>†</sup>

Department of Chemistry, University of Houston, Houston, Texas 77204-5641, U.S.A.

Received September 9, 1992

The neutral, reduced, and oxidized 2,2-trans isomers of  $\text{Rh}_2(\text{ap})_4$  (ap=2-anilinopyridinate) were investigated with respect to dioxygen binding in  $\text{CH}_2\text{Cl}_2$  containing 0.1 M tetrabutyl-ammonium perchlorate.  $\text{Rh}_2(\text{ap})_4$  binds dioxygen in nonaqueous media and forms a  $\text{Rh}^{\text{II}}\text{Rh}^{\text{III}}$  superoxide complex,  $\text{Rh}_2(\text{ap})_4(\text{O}_2)$ . This neutral species was isolated and is characterized by UV-visible and IR spectroscopy, mass spectrometry and cyclic voltammetry. It can be reduced by one electron at  $E_{1/2} = -0.45$  V vs. SCE in  $\text{CH}_2\text{Cl}_2$  and gives  $[\text{Rh}_2(\text{ap})_4(\text{O}_2)]^-$  as demonstrated by the ESR spectrum of a frozen solution taken after controlled potential reduction. The superoxide ion in  $[\text{Rh}_2(\text{ap})_4(\text{O}_2)]^-$  is axially bound to one of the two rhodium ions, both of which are in a +2 oxidation state.  $\text{Rh}_2(\text{ap})_4(\text{O}_2)$  can also be stepwise oxidized in two one-electron transfer steps at  $E_{1/2} = 0.21$  V and 0.85 V vs. SCE in  $\text{CH}_2\text{Cl}_2$  and gives  $[\text{Rh}_2(\text{ap})_4(\text{O}_2)]^+$  followed by  $[\text{Rh}_2(\text{ap})_4(\text{O}_2)]^{2+}$ . ESR spectra demonstrate that the singly oxidized complex is best described as  $[\text{Rh}^{\text{II}}\text{Rh}^{\text{III}}(\text{ap})_4(\text{O}_2)]^+$  where the odd electron is delocalized on both of the two rhodium ions and the axial ligand is molecular oxygen.

### Introduction

$\text{Rh}_2(\text{ap})_4$  (where ap=2-anilinopyridinate) can exist in four different isomeric forms, two of which have been isolated and structurally characterized.<sup>1,2</sup> The 4,0 isomer has one rhodium ion bound by four anilino nitrogens and the other by four pyridyl nitrogens. In contrast, each rhodium atom of the  $\text{Rh}_2(\text{ap})_4$  2,2-trans isomer is bound in a *trans* fashion

by two pyridyl nitrogens and two anilino nitrogens of the bridging ligands.

Our laboratory recently reported electrochemical properties of the 4,0 isomer in the presence of  $\text{O}_2$  and demonstrated the formation of  $\text{Rh}^{\text{II}}\text{Rh}^{\text{III}}(\text{ap})_4(\text{O}_2)$ , where the dioxygen ligand was bound to the rhodium ion which was complexed by the four pyridyl nitrogens.<sup>3</sup> The 2,2-trans isomer of  $\text{Rh}_2$ , whose structure is shown in Figure 1, will also irreversibly bind dioxygen and gives a stable  $\text{Rh}_2(\text{ap})_4(\text{O}_2)$  complex in  $\text{CH}_2\text{Cl}_2$  or THF solutions under  $\text{O}_2$ . This complex was isola-

\*On leave of absence from Dong-A University, Korea.